

# On the occupation of X-ray selected galaxy groups by radio AGN since $z = 1.3^a$

V. Smolčić<sup>1,2,3</sup>, A. Finoguenov<sup>4,5</sup>, G. Zamorani<sup>6</sup>, E. Schinnerer<sup>7</sup>,  
M. Tanaka<sup>8,2</sup>, S. Giodini<sup>9</sup>, N. Scoville<sup>10</sup>

<sup>a</sup>Based on observations with the National Radio Astronomy Observatory which is a facility of the National Science Foundation operated under cooperative agreement by Associated Universities, Inc.; the XMM-Newton, an ESA

science mission with instruments and contributions directly funded by ESA Member States and NASA

<sup>1</sup>ESO ALMA COFUND Fellow

<sup>2</sup>European Southern Observatory, Karl-Schwarzschild-Strasse 2, D-85748 Garching b. München, Germany

<sup>3</sup>Argelander Institut für Astronomie, Auf dem Hügel 71, Bonn, D-53121, Germany

<sup>4</sup>Max-Planck-Institut für Extraterrestrische Physik, Giessenbachstraße, 85748 Garching, Germany

<sup>5</sup>University of Maryland, Baltimore County, 1000 Hilltop Circle, Baltimore, MD 21250, USA

<sup>6</sup>INAF - Osservatorio Astronomico di Bologna, via Ranzani 1, I-40127 Bologna, Italy

<sup>7</sup>Max-Planck-Institut für Astronomie, Königstuhl 17, D-69117 Heidelberg, Germany

<sup>8</sup>Institute for the Physics and Mathematics of the Universe, The University of Tokyo, 5-1-5 Kashiwanoha, Kashiwa-shi, Chiba 277-8583, Japan

<sup>9</sup>Leiden Observatory, Leiden University, PO Box 9513, 2300 RA Leiden, the Netherlands

<sup>10</sup>California Institute of Technology, MC 105-24, 1200 East California Boulevard, Pasadena, CA 91125

16 August 2011

## ABSTRACT

Previous clustering analysis of low-power radio AGN has indicated that they preferentially live in massive groups. The X-ray surveys of the COSMOS field have achieved a sensitivity at which these groups are directly detected out to  $z = 1.3$ . Making use of Chandra-, XMM- and VLA-COSMOS surveys we identify radio AGN members ( $10^{23.6} \lesssim L_{1.4\text{GHz}}/(\text{W Hz}^{-1}) \lesssim 10^{25}$ ) of galaxy groups ( $10^{13.2} \lesssim M_{200}/M_{\odot} \lesssim 10^{14.4}$ ;  $0.1 < z < 1.3$ ) and study i) the radio AGN – X-ray group occupation statistics as a function of group mass, and ii) the distribution of radio AGN within the groups. We find that radio AGN are preferentially associated with galaxies close to the center ( $< 0.2 \cdot r_{200}$ ). Compared to our control sample of group members matched in stellar mass and color to the radio AGN host galaxies, we find a significant enhancement of radio AGN activity associated with  $10^{13.6} \lesssim M_{200}/M_{\odot} \lesssim 10^{14}$  halos. We present the first direct measurement of the halo occupation distribution (HOD) for radio AGN, based on the total mass function of galaxy groups hosting radio AGN. Our results suggest a possible deviation from the usually assumed power law HOD model. We also find an overall increase of the fraction of radio AGN in galaxy groups ( $< 1 \cdot r_{200}$ ), relative to that in all environments.

**Key words:** galaxies: active, – cosmology: observations – radio continuum: galaxies

## 1 INTRODUCTION

The general interest in radio AGN has increased in the last years as their energy outflows both, theoretically and observationally substantiate feedback processes highly relevant for massive galaxy formation, and galaxy cluster/group physics (e.g. Croton et al. 2006, Bower et al. 2006, Smolčić et al. 2009; Smolčić 2009, Smolčić & Riechers 2011, Giodini et al. 2009, 2010). Studies of low radio power (predominantly low-excitation, i.e. with weak or absent emission lines in their optical spectra) AGN have shown that the probability of finding a radio AGN is a strong function of stellar

mass of the host galaxy (e.g. Best et al. 2005, Smolčić et al. 2009). At high stellar masses ( $M_{*} \sim 10^{12} M_{\odot}$ ) this probability approaches unity for galaxies out to  $z = 1.3$  (Smolčić et al. 2009). As high stellar mass galaxies usually reside in group/cluster environments (e.g. Mandelbaum et al. 2006; Leauthaud et al. 2010), it is still not entirely clear whether it is the host galaxy and/or environmental properties that determine the nature of radio AGN.

Initially, Ledlow & Owen (1996) found no differences between the bivariate radio-optical luminosity function for radio AGN in the cluster and in the field, suggesting that

cluster environment does not play a major role in radio AGN triggering. However, using a sample of radio AGN drawn from the NVSS (NRAO VLA Sky Survey; Condon et al. 1998) and comparing the radio luminosity functions in (ROSAT selected X-ray) clusters and in the field Lin & Mohr (2007) found a factor of 6.8 higher probability of a galaxy being a radio AGN in the clusters than in the field ( $z < 0.0647$ ).

A detailed radio AGN clustering analysis at  $z \sim 0.55$  has been performed by Wake et al. (2008). Constructing cross(auto)-correlation functions of  $0.4 < z < 0.8$  2SLAQ Luminous Red Galaxies (LRGs), NVSS radio detected LRGs and a control sample matched in redshift, color and optical luminosity to the radio AGN they found that radio AGN are significantly more clustered than the control population of radio-quiet galaxies. Assuming various models for the halo occupation distribution, they find that radio AGN typically occupy more massive halos compared to the control sample galaxies, suggesting that the probability of finding a radio AGN in a massive galaxy (at  $z \sim 0.55$ ) is influenced by the halo mass and/or cluster environment.

It is important to stress that both clustering and stacking of halos, used in the above analyzes (Wake et al. 2008, Mandelbaum et al. 2009) suffer from degeneracies towards the distribution of radio AGN in halos, either based on uncertainties of halo occupation of massive galaxies (van den Bosch et al. 2004) or degeneracies of HOD modelling (e.g. Miyaji et al. 2011). Thus, optimally one would directly study the HOD by identifying the radio AGN within the galaxy groups. This can be done by using a well defined statistically significant sample of radio AGN and X-ray selected galaxy groups and clusters. In this Letter we make use of such a sample in the COSMOS field in order to directly study the halo occupation of radio AGN. We adopt  $H_0 = 71$ ,  $\Omega_M = 0.25$ ,  $\Omega_\Lambda = 0.75$ .

## 2 THE SAMPLES

The Cosmic Evolution Survey (COSMOS) is a panchromatic photometric and spectroscopic survey of  $2\frac{1}{2}^\circ$  of the sky observed by the most advanced astronomical facilities (e.g. VLA, Chandra, XMM-Newton, Subaru, CFHT; see Scoville et al. 2007). It allows a robust source identification and extended selection of various source types. The statistics on both radio AGN and selection of halos based on their X-ray emission enables a construction of a statistically significant catalog of radio AGN in massive halos, as described below.

### 2.1 Radio AGN and red galaxy control samples

We make use of the COSMOS radio AGN sample defined by Smolčić et al. (2008, see also Smolčić et al. 2009). It consists of  $\sim 600$  low-power ( $L_{1.4\text{GHz}} \lesssim 10^{25} \text{ W Hz}^{-1}$ ) radio AGN galaxies out to a redshift of  $z = 1.3$ . The sample was generated by matching the 20 cm VLA-COSMOS Large Project sources (Schinnerer et al. 2007) with the UV-NIR COSMOS photometric catalog (Capak et al. 2007). The selection required optical counterparts with  $i_{\text{AB}} \leq 26$ , accurate photometry, and a S/N  $\geq 5$  (i.e.  $\gtrsim 50 \mu\text{Jy}$ ) detection at 20 cm. The radio AGN hosts were identified as red galaxies based on a rest-frame optical color ( $P1$  color  $\geq 0.15$ ) that mimics the standard spectroscopic classification methods (see

Smolčić et al. 2006, 2008 for details). The rest-frame color method efficiently selects mostly type 2 AGN (such as LINERs and Seyferts), and absorption-line AGN (with no emission lines in the optical spectrum), while type 1 AGN (i.e. quasars,  $\lesssim 20\%$  of the total AGN sample) are not included (see Smolčić et al. 2008 for detailed definitions).

Furthermore, from the full COSMOS photometric redshift catalog (Ilbert et al. 2009), using the same optical magnitude, redshift and color selection criteria as for their radio-AGN, Smolčić et al. (2009) generated a control galaxy sample from which the radio AGN are drawn ("control sample" hereafter). Here we make use of both of these samples, and add two additional requirements. First, we use a luminosity limited sample of radio AGN ( $23.6 \leq \log L_{1.4\text{GHz}}/(\text{W Hz}^{-1}) \lesssim 25$ ;  $M_i \leq -22.5$ ) in order to avoid selection effects induced by limiting in flux rather than luminosity. Second, in order to disentangle the dependence of radio emission on the host stellar mass, we select a subsample of control galaxies ( $M_i \leq -22.5$ ) that i) are not detected at 20 cm, and ii) have a stellar mass distribution equivalent to that of our radio AGN. Given these two criteria we consider this sample to be "radio-quiet" and refer to it hereafter as "stellar mass matched control sample". Our criteria yield 217 galaxies in the radio AGN sample,  $\sim 5300$  in the control sample and 618 in the stellar mass matched control galaxy sample. The median redshifts of the radio and stellar mass matched control galaxy samples are 0.72 and 0.85, respectively. At stellar masses exceeding  $10^{12} M_\odot$ , we do not find galaxies without a radio AGN.

### 2.2 X-ray sample of galaxy groups

The COSMOS field has been subject of intensive X-ray observations by XMM-Newton (Hasinger et al. 2007; Cappelluti et al. 2009) and Chandra (Elvis et al. 2009). Following the method of Finoguenov et al. (2009) a detailed subtraction of point sources was performed, which allowed us to substantially reduce the contamination level of the catalog and to improve the localization of the center of extended X-ray emission. We use the complete set of XMM-Newton observations, described in detail in Cappelluti et al. (2008). We also added the data of the Chandra-COSMOS survey (Elvis et al. 2009), after the removal of point sources. Identification of sources using the improved COSMOS photometric redshift catalog (Ilbert et al. 2009) is complete at all redshifts. Furthermore, the zCOSMOS-BRIGHT (Lilly et al. 2009) program provides spectroscopic identification for a dominant fraction (67%) of galaxies with  $i_{\text{AB}} \leq 22.5$  and  $z < 1$ . Most importantly, the mass-luminosity relation for the new sample of X-ray groups has been directly calibrated by Leauthaud et al. (2010) using weak lensing. If the systematic uncertainties of groups hosting radio AGN are consistent with those of the entire sample, then the systematic uncertainties are within 10% (Leauthaud et al. 2010). The X-ray group catalog contains 210 systems at redshifts below 1.3 with 130 groups having at least two spectroscopic redshifts that match the redshift of the red sequence.

### 2.3 Matching radio AGN and control samples to X-ray galaxy groups

We have cross-correlated the X-ray galaxy group catalog (see Sec. 2.2) with the i) full control sample, ii) stellar mass matched control sample, and iii) radio AGN sample (see Sec. 2.1). The correlation was done in projected 2D space as accurate redshifts are assigned for all samples. We perform the matching for each radio AGN/control galaxy by searching for the nearest cluster within a redshift slice centered at the galaxy's redshift  $z$ . We take the half-width of the redshift slice to be  $\Delta z = 0.0334 \cdot (1 + z)$ , which corresponds to  $\sim 3$  standard deviations of the COSMOS photometric redshift distribution for  $i < 24$  (see Ilbert et al. 2009 for details). Prior to imposing a limit on the distance between the radio AGN/control galaxy and the galaxy group center, below we consider the surface number density of radio AGN inside groups.

## 3 RESULTS

### 3.1 Surface density profile of radio AGN in galaxy groups

We derive the surface density profiles of the radio AGN and stellar mass matched control samples satisfying our selection criteria ( $\log L_{1.4\text{GHz}} \geq 23.6$  [W/Hz];  $M_i \leq -22.5$ ;  $P1 \geq 0.15$ ). The profiles have been computed as distance to the X-ray center in units of  $r_{200}$ <sup>1</sup> averaging over all the X-ray galaxy groups in our sample (with photometrically masked regions taken into account). In Fig. 1 we show the surface density profiles for our radio AGN and stellar mass matched control sample galaxies, scaled by a factor of 2.85 downward to account for the larger sample of the second relative to the first. There is a clear enhancement of occurrence of radio AGN at group centers ( $< 0.2 \cdot r_{200}$ ). This is consistent with results in the local universe ( $z < 0.0647$ ; Lin & Mohr 2007), and will be further discussed in Sec. 4.

### 3.2 Stellar mass function of radio AGN in galaxy groups: Effect of group environment on radio AGN triggering

In the upper panel of Fig. 2 we show the stellar mass function computed using the  $1/V_{\text{max}}$  method (see Smolčić et al. 2009 for details) of both radio AGN and control galaxies (not matched in stellar mass) that occupy all environments and galaxy groups ( $\leq 1 \cdot r_{200}$ ). It is noteworthy that in the highest mass bin ( $M_* \sim 10^{12} M_\odot$ ) essentially all red galaxies are radio AGN that tend to occupy galaxy groups. Dividing the stellar mass function of radio AGN by that of the control galaxy sample yields the volume corrected fraction of radio AGN relative to red host galaxies in all environments and in groups. This is shown in the bottom panel of Fig. 2. These fractions can be considered as probabilities that a massive red galaxy is a radio AGN in all and group ( $\leq 1 \cdot r_{200}$ ) environments, respectively. From Fig. 2 it is obvious that the fraction of radio AGN is enhanced in galaxy groups. In

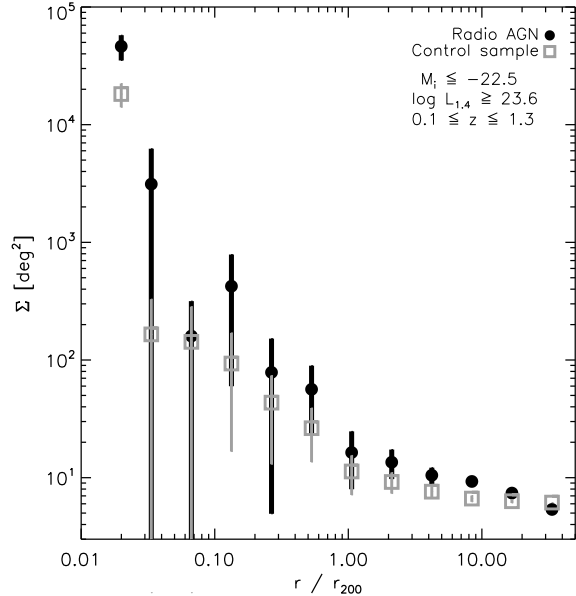


**Figure 1.** The surface density distribution for our radio AGN ( $L_{1.4\text{GHz}} \gtrsim 4 \times 10^{23}$  W/Hz; filled dots), and stellar mass matched control (open squares) galaxies. Both samples are volume limited in the optical ( $M_i \leq -22.5$ ). The profile for the stellar mass matched control sample has been normalized by dividing it by a factor of 2.85 (corresponding to the ratio between the numbers of galaxies in the stellar mass matched control sample and the radio AGN sample).

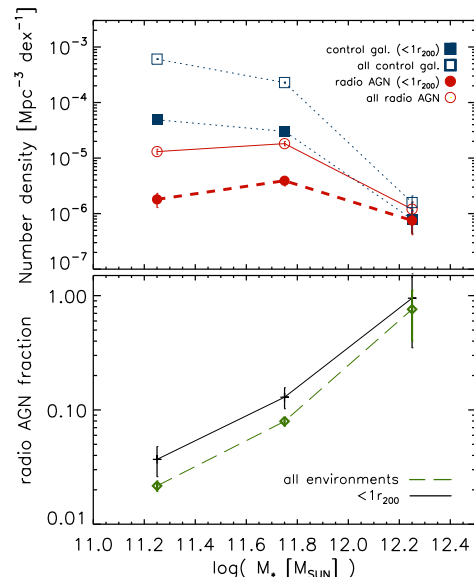


**Figure 2.** Top panel: stellar mass function for radio AGNs (red circles), red control galaxies (blue squares) within  $1r_{200}$  of group centres (filled symbols) and in all environments (open symbols). Bottom panel: fraction of radio AGNs (red circles) relative to red control galaxies in groups ( $\leq 1r_{200}$ ; solid line) and in all environments (dashed line).

the highest mass bin ( $10^{12.3} M_\odot$ ) the fraction of radio AGN is consistent with 1 irrespective of environment. At lower stellar masses ( $10^{11.8}$  and  $10^{12.3} M_\odot$ ) the enhancement of the fraction of radio AGN in groups is a factor of  $\sim 1.7$  and  $1.6$  respectively. These results imply that the triggering of radio AGN is directly linked to group environment.

<sup>1</sup>  $r_{200}$  is defined as the radius within which the average density equals 200 times the critical density. Accordingly,  $M_{200}$  is the total mass embedded within  $r_{200}$ . The values for the COSMOS sample are taken from Finoguenov et al. (2009).

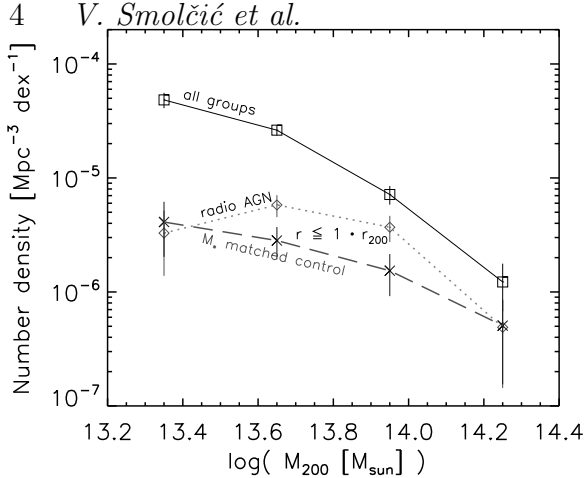


**Figure 3.** Differential mass function of X-ray galaxy groups. Squares indicate the full mass function. Diamonds show the mass function of groups hosting a radio AGN within  $1 \cdot r_{200}$ . Crosses show the mass function of groups hosting a massive radio-quiet (stellar mass matched control sample) galaxy.

### 3.3 Radio AGN in galaxy groups: Halo mass function and halo occupation distribution

In Fig. 3 we show the total mass function of all galaxy groups, and those hosting a radio AGN or a stellar mass matched control sample galaxy within  $1 \cdot r_{200}$ . Since the radio sample is volume-limited, in calculating the mass function we used the volume calculation ( $1/V_{\text{max}}$ ) for the X-ray group sample.

The shape of the total mass function of groups hosting a massive radio-quiet (i.e. stellar mass matched control sample) galaxy within  $1 \cdot r_{200}$  differs from that of all groups. Massive radio-quiet galaxies tend to occupy higher mass groups with increased frequency. On the other hand, groups hosting a radio AGN galaxy ( $L_{1.4\text{GHz}} \geq 10^{23.6} \text{ W Hz}^{-1}$ ) show a very different distribution with a preference for high-mass halos ( $\log(M_{\text{tot}}/M_{\odot}) \gtrsim 13.5$ ), in particular in the range of  $\log(M_{\text{tot}}/M_{\odot}) \sim 13.5 - 14.1$ , compared to the halo mass function of radio-quiet hosts. This enhancement in number density (relative to a stellar-mass matched sample) shows that the radio-AGN phenomenon (at least in the given  $M_{200}$  range) must be governed by a factor other than stellar mass.

Our data-set allows us to generate the halo occupation distribution (HOD), which describes the occupancy of dark matter halos by galaxies, directly. We simply need to divide the mass function of X-ray groups hosting radio AGN within  $1 \cdot r_{200}$  by that of all X-ray groups (see Fig. 3). As shown in Fig. 4, the HOD of radio AGN ( $\log L_{1.4\text{GHz}}/(\text{W Hz}^{-1}) \geq 23.6$ ) within  $1 \cdot r_{200}$  increases with total halo mass (embedded within  $r_{200}$ ).

It is conventional to fit the HOD with a power law. The best fit to our data assuming an  $\alpha(\frac{M}{10^{13.6} M_{\odot}})^{\beta}$  model yields  $\alpha = 0.16(0.13 - 0.19)$  and  $\beta = 0.90(0.65 - 1.14)$ , where the 68% confidence interval is given in brackets. The increase of the HOD with halo mass implies that the occurrence of radio AGN in higher mass halos is more frequent, compared to that in less massive ones. Such a result is consistent with that found by Wake et al. (2008).

Wake et al. (2008) have used a sample of 2SLAQ Luminous Red Galaxies (LRGs) at redshifts 0.4-0.8, combined with FIRST and NVSS 20 cm radio data to study the clustering properties of the i) full LRG sample, ii) radio

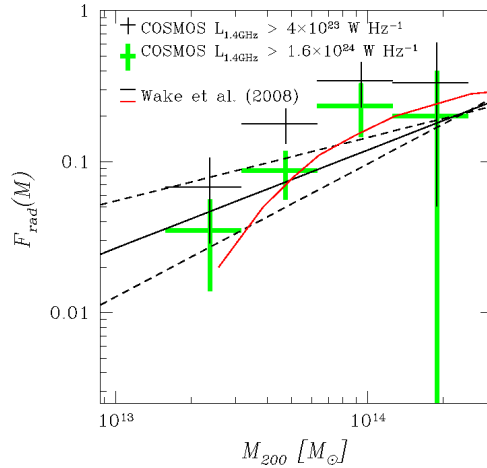


**Figure 4.** Occupation of X-ray selected groups by weak radio AGN. The COSMOS results (black:  $L_{1.4\text{GHz}} \gtrsim 4 \times 10^{23} \text{ W Hz}^{-1}$ , gray:  $L_{1.4\text{GHz}} \gtrsim 1.6 \times 10^{24} \text{ W Hz}^{-1}$ ) are shown as crosses, indicating the mass range on the X-axis and statistical (68% confidence level) errors on the Y-axis. The results of Wake et al. (2008), assuming a power-law dependence of radio-fraction, are shown as solid line (best fit) and short-dashed line (68% confidence interval). The solid curve shows the results of Wake et al. (2008) obtained by dividing the best halo fits to the cross-correlation functions of their radio AGN and Luminous Red galaxies.

AGN with  $\log L_{1.4\text{GHz}} \geq 24.2[\text{W/Hz}]$ , and iii) radio-quiet LRGs matched in color, redshift, and optical luminosity to their radio-detected AGN. They fitted halo models to the constructed auto- (full LRG sample) and cross-correlation (radio-detected and matched LRGs) functions which allowed them to generate the radio AGN HOD. In Fig. 4 we compare the HOD of Wake et al. (2008), scaling their results to our mass definition and the value of the Hubble constant (Leauthaud et al. 2010).

The black (full and dashed) lines in Fig. 4 show their HOD modelling obtained from the best fit halo model to their control sample clustering. In their fitting the radio AGN fraction was left as a free parameter (assuming a power-law shape) to match the clustering and space density of radio detected LRGs. The red curve also shown in Fig. 4 was constructed by Wake et al. in a different way, by simply dividing their halo fits to the radio AGN and control sample data limited in luminosity. The parameters of our HOD fit (assuming  $\alpha(\frac{M}{10^{13.6} M_{\odot}})^{\beta}$ , and using only radio AGN more luminous than  $\sim 1.6 \times 10^{24} \text{ W Hz}^{-1}$ ) are  $\alpha = 0.09(0.06 - 0.11)$  and  $\beta = 0.86(0.45 - 1.22)$ , in agreement with those derived by Wake et al. (2008). The agreement in the HODs suggests no significant redshift evolution between 0.55 and 0.73 (corresponding to the median redshifts of the samples analyzed in Wake et al. and here, respectively). Furthermore, the deviant point at  $M_{200} \sim 10^{14} M_{\odot}$  suggests a non-power law form of the HOD as supported by the (red) curve in Fig. 4 (adopted from Wake et al. 2008). With a lower limiting radio power ( $\sim 4 \times 10^{23} \text{ W Hz}^{-1}$ ) we find that the HOD overall increases by a factor of 2-2.5, with a comparable slope to that given above.

## 4 SUMMARY AND DISCUSSION

Using well defined samples of low-power radio AGN (which are mainly hosted by massive early type galaxies; see e.g. Smolčić et al. 2008, 2009) and X-ray groups in the COS-

MOS field at redshifts  $z \leq 1.3$ , we analyzed the occupation of galaxy groups ( $10^{13.2} \lesssim M_{200}/M_{\odot} \lesssim 10^{14.4}$ ) by radio AGN ( $10^{23.6} \lesssim L_{1.4\text{GHz}}/(\text{W Hz}^{-1}) \lesssim 10^{25}$ ), as well as the effect of group environment on radio AGN. In order to investigate the latter, it is essential to separate the stellar mass and clustering effects. The blending of these two arises from the fact that i) the probability of a massive early type galaxy to host a radio AGN strongly rises with stellar mass (e.g. Best et al. 2005; Smolčić et al. 2009), and ii) massive red galaxies preferentially reside in clustered environments (e.g. Mandelbaum et al. 2006). To overcome this bias, we have constructed a control sample of radio-quiet galaxies, selected in the same way as our radio AGN, with a stellar mass distribution matched to that of our radio AGN. Thus, any differences in the derived distributions of these samples should arise due to effects other than stellar mass.

Generating surface density profiles for our radio AGN and radio-quiet stellar-mass matched control galaxies as a function of  $r_{200}$  (see Fig. 1) we find a strong enhancement of radio AGN in group centers ( $< 0.2 \cdot r_{200}$ ). This is consistent with the results in the local universe ( $z < 0.0647$ ; Lin & Mohr 2007). As our stellar mass matched control sample bypasses the stellar mass/clustering bias (contrary to that in Lin & Mohr 2007), our results directly link group environment to radio-AGN triggering. The effect of groups on radio AGN is also clearly demonstrated in Fig. 2, where we have shown that the fraction of radio AGN relative to red control galaxies is overall enhanced in galaxy groups.

Using the halo mass functions (derived from our X-ray data; see Fig. 3) we generated the halo occupation distribution of radio AGN (see Fig. 4). There is a very good agreement in the HOD results between our survey and Wake et al. (2008;  $L_{1.4\text{GHz}} \gtrsim 1.6 \times 10^{24} \text{ W Hz}^{-1}$ ), despite very different calculations. Generating auto/cross-correlation functions Wake et al. (2008) estimated the mass of the halos based on the observed bias (the discrepancy between the distribution of galaxies and the underlying dark matter). In our analysis the mass of the halo has been measured directly via weak lensing. Unlike the bias-mass relation, weak lensing masses do not depend on the assumed growth of structure. Moreover, our results allow to break the degeneracy of HOD models and suggest a complex (non-power law) shape of the occupational distribution for radio AGN.

As our radio data are deeper than that used in Wake et al. (2008) we have studied the HOD of radio AGN to lower radio powers ( $L_{1.4\text{GHz}} \gtrsim 4 \times 10^{23} \text{ W Hz}^{-1}$  which corresponds to a volume limited sample out to  $z = 1.3$ ). With such a cut the HOD of radio AGN overall increases by a factor of 2-2.5. The HOD can be interpreted as the probability that a massive red galaxy within  $1 \cdot r_{200}$  is a radio AGN. This probability can then be viewed as the fraction of time a massive galaxy spends as a radio AGN. Thus, it gives insights into the radio AGN duty cycle. Assuming that the red galaxy population was created at  $z \sim 2-3$  (i.e. 11 Gyrs ago) for  $L_{1.4\text{GHz}} \gtrsim 4 \times 10^{23} \text{ W Hz}^{-1}$  this yields an average time a massive red galaxy in a galaxy group spends as a radio AGN of about 0.7 Gyr at  $M_{200} \sim 2 \times 10^{13} M_{\odot}$  to  $\sim 4$  Gyrs at the high mass end ( $M_{200} \sim 10^{14} M_{\odot}$ ). If we restrain the elapsed cosmic time to the observed redshift range ( $0 < z < 1.3$ ) we obtain an average time scale of  $\sim 0.6 - 3.5$  Gyrs. If radio AGN triggering is caused by fueling of the supermassive black hole via cooling of the

large-scale hot gas Churazov et al. (2002), then the increase of the HOD with halo mass implies an overall higher fueling efficiency in high mass halos. In summary, our results yield that group environment enhances (on average by a factor of  $\sim 2$ ) the probability of a red massive galaxy being a radio AGN, and that radio AGN occupy higher mass halos with increased frequency.

## ACKNOWLEDGMENTS

This research was funded by the European Union's Seventh Framework programme under grant agreement 229517; and contract PRIN-INAF 2007. The XMM-Newton project is supported by the Bundesministerium fuer Wirtschaft und Technologie/Deutsches Zentrum fuer Luft- und Raumfahrt (BMWi/DLR, FKZ 50 OX 0001), the Max-Planck Society.

## REFERENCES

- Best, P. N., Kauffmann, G., Heckman, T. M., Brinchmann, J., Charlot, S., Ivezić, Ž., & White, S. D. M. 2005, MNRAS, 362, 25
- Bower, R. G., Benson, A. J., Malbon, R., Helly, J. C., Frenk, C. S., Baugh, C. M., Cole, S., Lacey, C. G. 2006, MNRAS, 370, 645
- Capak, P., et al. 2007, ApJS, 172, 99
- Cappelluti, N., et al. 2009, A&A, 497, 635
- Churazov E., Sunyaev R., Forman W., Böhringer H., 2002, MNRAS, 332, 729
- Condon, J. J., Cotton, W. D., Greisen, E. W., Yin, Q. F., Perley, R. A., Taylor, G. B., & Broderick, J. J. 1998, AJ, 115, 1693
- Croton, D. J., et al. 2006, MNRAS, 365, 11
- Elvis, M., et al. 2009, ApJS, 184, 158
- Finoguenov, A., et al. 2009, ApJ, 704, 564
- Giodini, S., et al. 2009, ApJ, 703, 982
- Giodini, S., et al. 2010, ApJ, 714, 218
- Hasinger, G., et al. 2007, ApJS, 172, 29
- Ilbert, O., et al. 2009, ApJ, 690, 1236
- Leauthaud, A., et al. 2010, ApJ, 709, 97
- Ledlow, M. J., & Owen, F. N. 1996, AJ, 112, 9
- Lilly, S. J., et al. 2009, ApJS, 184, 218
- Lin, Y.-T., & Mohr, J. J. 2007, ApJS, 170, 71
- Mandelbaum, R., Seljak, U., Kauffmann, G., Hirata, C. M., & Brinkmann, J. 2006, MNRAS, 368, 715
- Mandelbaum, R., Li, C., Kauffmann, G., & White, S. D. M. 2009, MNRAS, 393, 377
- Miyaji, T., Krumpe, M., Coil, A. L., & Aceves, H. 2011, ApJ, 726, 83
- Schinnerer, E., et al. 2007, ApJS, 172, 46
- Scoville, N., et al. 2007, ApJS, 172, 1
- Smolčić, V., et al. 2006, MNRAS, 371, 121
- Smolčić, V., et al. 2008, ApJS, 177, 14
- Smolčić, V., et al. 2009, ApJ, 696, 24
- Smolčić, V. 2009, ApJL, 699, L43
- Smolčić, V., & Riechers, D. A. 2011, ApJ, 730, 64
- van den Bosch, F. C., Norberg, P., Mo, H. J., & Yang, X. 2004, MNRAS, 352, 1302
- Wake, D. A., Croom, S. M., Sadler, E. M., & Johnston, H. M. 2008, MNRAS, 391, 1674